

Fig. 1. (A) Diakinesis showing 23 pairs (5 maize and 18 *Tripsacum*) of chromosomes. (B) Metaphase showing *Tripsacum* chromosomes at plates and early dissociation of ten maize chromosomes.

in this respect depending on the specific maize and *Tripsacum* stocks used (3). This report concerns hybrids which contains 36 *Tripsacum* and 10 maize chromosomes. The *Tripsacum* chromosomes regularly form 18 bivalents, while the maize chromosomes form 0 to 5 pairs. Maize chromosomes can be distinguished from *Tripsacum* chromosomes by their larger size (Fig. 1A). The maize pairs are not synchronized with the *Tripsacum* chromosomes and separate early. By the time the *Tripsacum* chromosomes line up on the metaphase plate, the maize chromosomes appear to be in a sort of suspended anaphase (Fig. 1B). The maize chromosomes may be included at random or more often excluded altogether in meiosis.

The 46-chromosome hybrids are male sterile, but when backcrossed to maize, the offspring are usually 46-chromosome plants resembling the F_1 morphologically. This is not due to apomixis because purple plants resembling the F_1 are recovered when the backcross is made to a maize genetic stock carrying the genes for purple plant color (*B*, *P1*). Evidently, the functional female gametes of the F_1

are primarily those with no maize chromosomes and the unreduced number (36) of *Tripsacum* chromosomes. The F_1 is reconstituted in each backcross generation. A few percent of the individuals in backcross populations have more than 46 chromosomes due to the inclusion of some maize chromosomes at meiosis. We have recovered plants with 50, 52, 54, and 56 chromosomes in backcross progenies.

The 56-chromosome plants are evidently derived from unreduced eggs of the hybrid and normal maize pollen. They contain 36 *Tripsacum* chromosomes that form 18 bivalents and 20 maize chromosomes that form 10 bivalents. Meiosis is almost completely regular in these plants, as expected. However, the 50-chromosome plants frequently form 25 bivalents. These are derived from 18 pairs of *Tripsacum* and seven pairs of maize. Of the seven maize pairs, four bivalents are to be expected as being those which would occur between the four extra maize chromosomes from the egg and their homologs within the set of ten chromosomes from the male parent. However, the remaining three maize pairs resulted from nonhomologous pairing among the remaining six chromosomes from the male parent. In these plants, the maize and *Tripsacum* chromosomes are well synchronized, and meiosis is regular. The seven pairs of maize chromosomes can be easily identified by size.

It is now apparent that in the right genetic environment (background), the ten chromosomes of maize will frequently form five pairs. Some might interpret this as evidence for a residual homoeology on the ground that the basic number in Maydeae and Andropogoneae is $X = 5$ rather than $X = 10$. Rhoades (4) has shown that maize chromosomes do contain duplicated re-

gions, but whether or not these represent vestiges of an ancient polyploidy has not yet been established. We are more inclined to interpret the pairing as nonhomologous and nonhomoeologous induced by the genetic background. We feel that all organisms that carry out meiosis have coded genetic information that orders the chromosomes to pair during meiosis. Asynaptic and desynaptic aberrations are mutations of such genetic information. The polyploid *T. dactyloides* ($2n = 72$) presumably carries a double dose of pairing orders, and, although autopolyploid in nature, the chromosomes associate regularly into bivalents. In this background chromosomes of the haploid maize genome pair with each other, and the 36 *Tripsacum* chromosomes associate into bivalents, but synchronization is off. In the 50-chromosome plants (36 *Tripsacum* chromosomes and 14 *Zea* chromosomes), the additional maize chromosomes probably carry additional genetic information specifically for the behavior of maize chromosomes, and a better balance of the chromosomal environment is achieved.

JACK R. HARLAN
J. M. J. DE WET
S. M. NAIK
R. J. LAMBERT

Crop Evolution Laboratory,
Agronomy Department,
University of Illinois, Urbana 61801

References and Notes

1. Y. C. Ting, *Cytologia* 31, 324 (1966); S. S. Chase, *Bot. Rev.* 35, 117 (1969); also our own observations.
 2. R. S. K. Chaganti, thesis, Harvard University (1965); P. C. Mangelsdorf and R. G. Reeves described a similar hybrid in *Texas Agr. Exp. Sta. Bull. No. 574* (1939).
 3. A comparison of 14 F_1 plants showed maize chromosomes forming no pairs in some plants and up to an average of 3.9 pairs in other plants. S. M. Naik, J. R. Harlan, R. J. Lambert, J. M. J. de Wet, in preparation.
 4. M. M. Rhoades, *Amer. Natur.* 85, 105 (1951).
- 6 November 1969

Neuroglia: Biophysical Properties and Physiologic Function

Abstract. *The membrane time constant of neocortical glial cells is about 385 microseconds, less than one-twentieth the known value for the Betz cell. Glial membrane specific resistance is low (approximately 200 to 500 ohm centimeters squared). Neuroglial cells are ideally suited to buffer the immediate extraneuronal space at areas of synaptic contact against the increases in external potassium ion concentration that accompany postsynaptic and spike activity and to minimize the spread of potassium ions to other pre- and postsynaptic regions.*

The protoplasmic astrocyte is the principal neuroglial cell within the gray matter of the normal brain (1). These cells possess an irregular cell body from

which numerous slender processes radiate to form differing relationships with capillaries, other astrocytes, and the receptive surfaces of neurons (2).

Though neuroglial cells may subserve supportive, nutritive, and reparative functions for nervous tissue, and perhaps metabolize neurotransmitters (3), there has been much interest as to whether they electrically isolate neural receptive sites from one another (1, 2, 4, 5) or promote information transfer (6).

Kuffler and co-workers (5) have established that neuroglial cells in leeches, amphibians, and mammals have high resting potentials (often -75 to -90 mv), are selectively permeable to K^+ , and are electrically inexcitable. They may be depolarized as a consequence of the release of K^+ by neighboring neurons during either postsynaptic or spike activity, and some current may flow from one glial cell into another through a low resistance pathway thought to be provided by gap junctions (7).

Cells in the cat cortex showing most of these properties (8, 9) have now been identified as glial cells by marking techniques (10, 11). We have determined glial membrane electrical constants; the values obtained allow resolution of a number of difficulties in the interpretation of glial function.

Five cats were anesthetized with pentobarbital (35 mg/kg). Methods for preparing the animal, reducing cortical pulsations, and utilizing a Wheatstone bridge to permit simultaneous stimulation through and recording from fine glass micropipettes filled with 2M potassium-citrate have been described (12). The electrical activity was led through a short chlorided silver wire to a driven shield Microdot cable and then to a high input impedance amplifier (Picometric amplifier, Instrumentation Laboratory) that had low noise and fast rise time. Electrode "switching" artifacts attending the "make" and "break" of rectangular current pulses were kept to between 150 and 175 μ sec by using the lowest resistance (8 to 12 megohms) electrodes that could satisfactorily impale glial cells. Electrodes were checked for distorting artifacts before and after intracellular study by passing current pulses of the same intensities that were used during the intracellular study. Slope analysis was restricted to the period following subsidence of the "make" artifacts (Fig. 1A), and a method was devised for computing input resistance from slope and applied current measurements, which are made independently of the "balance" position of the bridge trace. Thus errors due to electrode artifacts and bridge

Table 1. Values of resting membrane potential, time constant, and input resistance for cortical neuroglial cells ranked in order of increasing resting potential.

Cell No.	V_R (mv)	τ (μ sec)	R_I (megohm)
1	-50	411	18.8
2	-55	338	13.1
3	-58	632	9.2
4	-63	442	11.0
5	-65	217	15.9
6	-65	377	7.8
7	-66	347	5.9
8	-72	478	4.7
9	-74	328	5.8
10	-76	354	6.6
11	-77	457	12.0
12	-78	384	12.7
13	-80	352	19.6
14	-87	307	4.5
15	-92	347	9.8
\bar{X}	-70.5	384.7	10.49
\pm S.D.	11.7	93.9	4.88

imbalance have been eliminated. Analysis has been restricted to 15 neuroglial cells with stable resting potentials of at least -50 mv. These cells were recorded from the neocortex as judged from micromanipulator depth readings of 50 to 1500 μ m and from the fact that, even after study of the deepest cells, neurons could still be impaled at slightly deeper penetration. Sensorimotor and sensory association cortices were studied. The usual assumptions that are made for analysis of current-voltage changes across the parallel resistance and capacitance of cell membranes have been described elsewhere (12).

Resting potentials ranged from -50 to -92 mv and averaged -70.5 ± 11.5 mv (Table 1). The membrane time constant was determined by slope analysis (12) of the membrane voltage changes in response to rectangular current pulses (Fig. 1, A and E). In all cases, the plot of $(\log dV/dt)$ versus t was linear, satisfying a differential equation for an exponential curve,

$$dV/dt = V_M/\tau \cdot e^{-t/\tau}$$

where V is voltage, V_M is the maximum voltage reached at times $t \gg \tau$, t is time, and τ is the membrane time constant.

Representative traces were projected onto the face of a Tektronix 565 scope, on which was also displayed the exponential charging curve generated across a "dummy" cell consisting of a resistance and a capacitance in parallel. The scope time base and the current in-

tensity supplied to the dummy cell were modified until an almost perfect fit was obtained in every case (Fig. 1B). Good exponential fits were not obtained for neurons (Fig. 1, C and F) in which the conductance of the profusely branched dendritic trees dominates the conductance of the soma; for these neurons the cable equation applies (12, 13).

The glial time constant ranged from 217 to 632 μ sec and averaged 384.7 ± 93.9 μ sec. Individual values are listed in Table 1. There was no difference in the values obtained with depolarizing and hyperpolarizing pulses. No active (regenerative) responses were seen, even when the membrane was depolarized by 50 mv. There was no evidence of either slow membrane potential shifts or a "second" membrane time constant when current pulses were applied to neuroglial cells for durations of approximately 100 times the passive membrane time constant (Fig. 1C).

After the time constant was determined, the input resistance (R_I) was calculated from the expression

$$R_I = \tau/I_A \cdot (dV/dt_{t=0})$$

derived from the previous equation and Ohm's law, where I_A is the applied current and $(dV/dt_{t=0})$ is the slope at $t=0$ determined by extrapolating the linear $(\log dV/dt)$ versus t relationship back to time zero. Thus R_I can be determined independently of any uncertainty in the positioning of the bridge balance trace. For individual cells R_I ranged from 4.5 to 19.6 megohms and averaged 10.49 ± 4.88 megohms (Table 1). Current-voltage relationships in the physiologic voltage range were linear (Fig. 1D).

Six of the fifteen cells had resting potentials from -76 to -92 mv, a range well above the range for neurons (12). This finding is in accord with results of workers who have studied neurons and glia in the same preparation (5, 10); the high value is in keeping with a membrane almost exclusively permeable to K^+ .

The extremely short membrane time constant (384.7 μ sec) is less than 1/20th of the value for the Betz cell (12) but is of the same order as the falling phase of the neocortical action potential, the phase of highest K^+ conductance (Fig. 1C). The glial time constant falls within one standard deviation of the value (311 ± 84 μ sec) recently found for human fetal astrocytes in tissue culture (14). These workers measured the surface area of cells

by photomicrographic planimetry and checked for the limits of accuracy of this technique by electron micrographic study of sister cultures. From their data on surface area, input resistance, and time constant, they calculated the membrane specific capacity as 0.8 to 2.0 $\mu\text{f}/\text{cm}^2$. Taking this range of values of specific capacity as applicable to the feline glial cell whose average time constant is 384.7 μsec , we estimate the specific resistance (R_m) of the cat glial membrane to be 193 to 482 ohm cm^2 . The higher value of R_m is probably a safe upper limit, because membrane specific capacity (C_s) has rarely been found significantly less than 0.8 $\mu\text{f}/\text{cm}^2$ (15) and because $R_m = \tau/C_s$. Thus, the ionic conductance, the reciprocal of the specific resistance, which for the glial cell is almost entirely a K^+ conductance, is very high, no less than 2.07×10^{-6} amp/ cm^2 mv or 1.29×10^{13} K^+ ion/sec cm^2 mv.

Neuroglial cells in the brain register depolarizations of up to 5 mv during the rhythmic 10/sec spindle bursts (10) and up to 20 mv during intense synaptic bombardment of cortical neurons (9). From the Nernst equation, at 37°C a resting potential of -92.9 mv would result if the intracellular and extracellular K^+ concentration is 100 and 3 mmole/liter, respectively (5). Addition of 1 mmole of K^+ per liter to a 250-Å extracellular space adds 1.5×10^{12} K^+ ion/ cm^2 of opposed glial membrane,

which depolarizes the membrane by 7.6 mv. [Each action potential of the squid axon can add a similar amount of K^+ (16).] During 10/sec spindles, if K^+ is released about equally during both the excitatory and inhibitory phases of the cycle, then 3×10^{13} K^+ ion/ cm^2 sec are released into the extracellular space. Taking the previous values of the K^+ conductance and a voltage change of 7.6 mv, we calculate that a current of approximately 9.8×10^{13} K^+ ion/ cm^2 sec is initiated, which is ample to carry away the buildup of K^+ . The safety factor is actually greater than the ratio 9.8:3 because K^+ would be continuously carried away before such concentrations could build up.

Though no precise estimate for the extracellular redistribution of K^+ across a glial process can be made owing to the lack of dimensional data, a *least spread* estimate is possible. The smallest glial processes taper into lamellar sheets of thickness 200 to 1000 Å (17). For a rectangular sheet of thickness d , small with respect to its width, the length constant

$$\lambda = [(d/2) \cdot (R_m/R_i)]^{1/2}$$

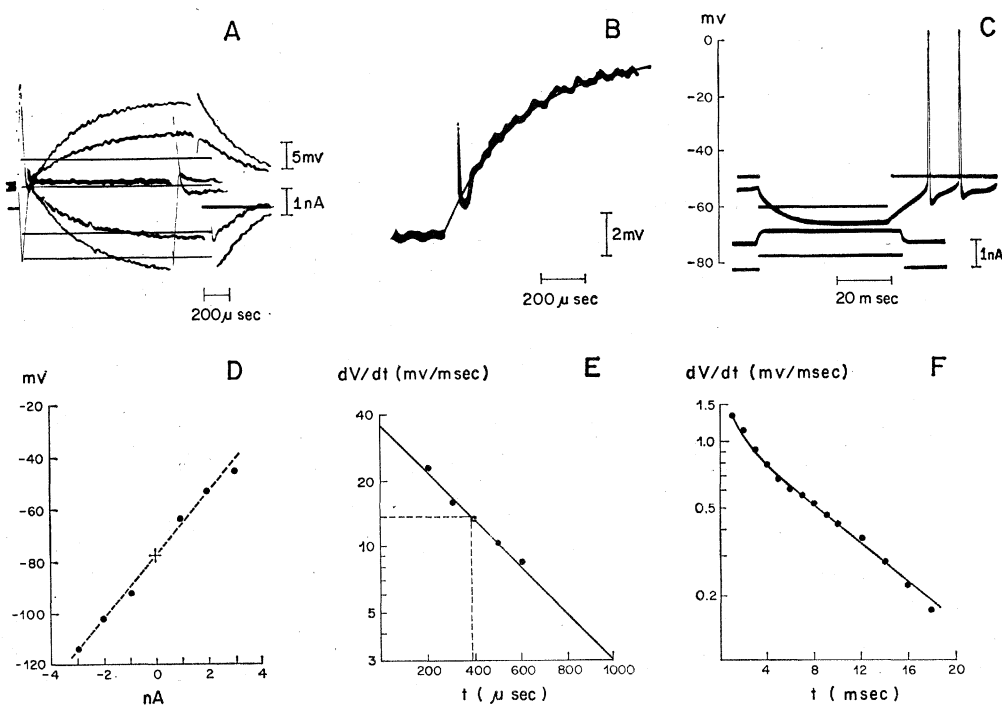
which is $(2)^{1/2}$ times greater than the value given for a cylinder of diameter d (13). Therefore, λ for a 200-Å sheet would not be less than 18.4 μm , taking R_m as 200 ohm cm^2 and R_i as 60 ohm cm (18). No cross-sectional

value of λ will be less than 18.4 μm because the lamellar sheets expansively broaden centripetally.

For a cylindrical process of infinite extent under steady-state conditions, transmembrane current loss and voltage decay occur proportionally, and $V = V_0 e^{-x/\lambda}$ (13). For a least spread of current calculation, the input resistance of an average neuroglial cell (about 10 megohms, Table 1) will be "redistributed" along an equivalent reference cylinder of infinite extent with a diameter [derived from Rall's equation 10 (13, p. 499)] of 3.7 μm . This procedure is reasonable provided that most of the cell's input resistance is distributed at a large distance from the process termination, a situation that is supported by anatomic data (1). The length constant of the reference cylinder using comparable values of R_i and R_m would be 170 μm .

Because this value of λ is so much greater than that for the glial terminal, the voltage at points along terminal processes (of diameter $< 3.7 \mu\text{m}$) will be underestimated in calculations that use the value 18.4 μm for λ and that are based on the above expression for exponential decay. Similarly, the percentage of the total current dropped beyond a given point will be underestimated. For example, no less than 76 percent of the current crosses the glial membrane at distances greater than 5 μm , a length about 200 times the width

Fig. 1. (A) Voltage responses of a cortical neuroglial cell to rectangular current pulses. Extracellular control recordings to ± 1 -na pulses have been superimposed as center set of traces. Resting membrane potential is -78 mv. (B) Parallel resistance-capacitance network match (fine line) of the charging curve of a neuroglial cell at high gain. Match is almost perfect after subsidence of electrode artifact. (C) Charging curves of neuron (above) and glial cell (below) to rectangular current pulses in the hyperpolarizing and depolarizing direction, respectively. (D) Linear current-voltage relationship for cell shown in (A). Cross indicates resting membrane potential. (E) Semilog plot of (dV/dt) versus (t) of a glial cell to a 1-na rectangular current pulse. The plotted points fit a straight line which can be regressed to $t = 0$. At $1/e \cdot dV/dt|_{t=0}$, $t = \tau$. (F) Semilog plot of (dV/dt) versus (t) for unidentified neuron in posterior sigmoid cortex shown in (C). Note initial deviations from linearity.



of the extracellular space. Therefore, even the finest glial processes permit distribution of large amounts of K^+ at significant distances from the extracellular spaces closest to areas of synaptic contact.

As the principal extracellular cation is Na^+ , the return current through the extracellular spaces largely replaces K^+ with Na^+ . Under these conditions, glia do not take up K^+ ; rather they transport it from the most K^+ -sensitive regions near presynaptic terminals and postsynaptic sites to more remote extracellular loci. The K^+ moves until extracellular inequalities are abolished. In the process the leaked K^+ becomes more evenly distributed and diluted in a relatively large volume of extracellular space (5).

The voltage distribution along glial sheets described above differs from the voltage distribution for the dendrites of neocortical cells, which are both much wider in diameter and of much higher membrane specific resistance (12, 19). The fine glial sheets are poorly suited for spread of potentials over distances comparable to those involved in dendritic electrotonic propagation (100 to 1000 μm) (19). [Relative neuronal and neuroglial contributions to cortical surface potentials have been analyzed (20).]

The glial time constant (385 μsec) is well suited for the membrane conductance to transfer the leaked K^+ attending the falling phase of the spike (420 μsec) (12) of neighboring neurons. Once the firing level of a neuron is reached, very slight changes in current entering the cell produce very great changes in the firing frequency (21). Thus one of the most exquisitely sensitive signaling prerogatives of highly integrative neurons is protected by the glial processes that ensheath them.

The limiting values for the three variables (τ , R_m , and λ) that control the speed, magnitude, and extent of K^+ movement across glial membranes have now been determined. These data provide a quantitative basis for glial cells serving as "spatial buffers" in the distribution of K^+ in the cleft system" as originally suggested by Orkand, Nicholls, and Kuffler (5). Moreover, the value of R_m seems suited for an optimal balance between rapid uptake and transport of K^+ . A lower value of R_m would result in a greater K^+ current for any given voltage generated across a glial process but a shorter "length constant" and a more limited movement of K^+ from critical regions.

A greater value of R_m would inversely decrease the K^+ current.

Stabilization of the K^+ concentration around the presynaptic terminals, where packets of transmitter are released onto neurons, is also of great importance. At the neuromuscular junction, the frequency of miniature end plate potentials increases with external K^+ concentration, particularly as concentrations rise above 10 mM (22). The glial investments that enclose fiber terminals in brain not only buffer such terminals and the postsynaptic membranes from the K^+ released by both pre- and postsynaptic activity but also limit spread to and from other areas of synaptic contact.

The passive transport system would break down when a glial cell and its processes become bathed uniformly. When large accumulations of K^+ are released during intensive and prolonged neural activity, the K^+ "pumps" described by Hertz (6) and others would be of prime importance in reducing the extracellular K^+ (see also (23)). Flow of K^+ into neighboring glial cells through gap junctions and into capillaries and cerebrospinal fluid would now be mechanisms for K^+ redistribution.

Anatomists have suggested that afferent fibers carrying similar information are segregated into the same compartments by neuroglial sheets or cuffs (2, 24). The consequences of an overload of extracellular K^+ are first restricted to those compartments in which overload was initiated. Keeping lost K^+ close by may facilitate later uptake by these fibers and neurons (see also 25).

Peters and Palay (2) have proposed as a general principle that the fine processes of astrocytes are so arranged "that receptive surfaces of neurons are insulated from all axonal terminals except those that synapse specifically upon them." The extent of glial investment is related to the complexity of the synaptic arrangement. At the electron micrographic level they find agreement for the isolating role of neuroglia proposed by Cajal (1) over 60 years ago from light microscopic observations. Our findings now provide a physiologic explanation of the isolating process and an appreciation of the great precision by which the neuroglial K^+ "spatial buffering" system (5) ensures the functional integrity of the synaptic mode of information transfer within the neuropile of the normal brain.

Finally, though these results pertain to astroglia of the mammalian neocortex with its complex integrative requirements, the evaluation of neuroglial functions at other loci and in other classes must depend on the specific structural and integrative requirements of those nervous structures (25).

MICHAEL C. TRACHTENBERG*

DANIEL A. POLLEN

Neurobiology Laboratory, Neurosurgical Service, Massachusetts General Hospital, Boston 02114

References and Notes

1. S. R. Cajal, *Histologie du Système Nerveux de l'Homme et des Vertébrés*, translated by L. Azoulay (Maloine, Paris, 1909), pp. 248-249.
2. A. Peters and S. L. Palay, *J. Anat.* **99**, 419 (1965); S. L. Palay, in *Nerve as a Tissue*, K. Rodahl and B. Issekutz, Eds. (Harper & Row, New York, 1966), pp. 4-10.
3. G. B. Koelle, *J. Pharmacol. Exp. Ther.* **114**, 167 (1955).
4. J. D. Green, D. S. Maxwell, H. Petsche, *Electroencephalogr. Clin. Neurophysiol.* **13**, 854 (1961); C. P. Wendell-Smith and M. J. Blunt, *Nature* **208**, 600 (1965).
5. S. W. Kuffler and J. G. Nicholls, *Ergeb. Physiol.* **57**, 1 (1966); — and D. D. Potter, *J. Neurophysiol.* **27**, 290 (1964); R. K. Orkand, J. G. Nicholls, S. W. Kuffler, *ibid.* **29**, 788 (1966); M. J. Dennis and H. M. Gerschenfeld, *J. Physiol. (London)* **203**, 211 (1969).
6. L. Hertz, *Nature* **208**, 1091 (1965); R. Galambos, *Proc. Nat. Acad. Sci. U.S.A.* **47**, 129 (1961); H. Hydén and E. Egyházi, *ibid.* **49**, 618 (1963); J. Cummins and H. Hydén, *Biochim. Biophys. Acta* **60**, 271 (1962).
7. M. W. Brightman and T. S. Reese, *J. Cell Biol.* **35**, 16A (1967); *ibid.* **40**, 648 (1969); A. Peters, *J. Anat.* **96**, 237 (1962).
8. C. G. Phillips, *Quart. J. Exp. Physiol. Cogn. Med. Sci.* **41**, 58 (1956); C.-L. Li, *J. Neurophysiol.* **22**, 436 (1959).
9. Y. Karahashi and S. Goldring, *Electroencephalogr. Clin. Neurophysiol.* **20**, 600 (1966).
10. R. G. Grossman and T. Hampton, *Brain Res.* **11**, 316 (1968); R. G. Grossman, L. Whiteside, T. L. Hampton, *ibid.* **14**, 401 (1969).
11. S. Watanabe, G. Mitarai, S. Takenaka, *Int. Congr. Physiol. Sci. Proc. 24th* **7**, 459 (1968).
12. H. D. Lux and D. A. Pollen, *J. Neurophysiol.* **29**, 207 (1966).
13. W. Rall, *Exp. Neurol.* **1**, 491 (1969); *ibid.* **2**, 503 (1960).
14. M. C. Trachtenberg, P. Kornblith, J. Häuptli, in preparation.
15. K. S. Cole and H. J. Curtis, in *New Medical Physics*, O. Glasser, Ed. (Year Book, Chicago, 1950), vol. 2, p. 82.
16. R. D. Keynes and P. R. Lewis, *J. Physiol. (London)* **114**, 151 (1951).
17. J. Wolff, *Z. Zellforsch.* **66**, 811 (1965); G. D. Pappas, E. B. Cohen, D. P. Purpura, in *The Thalamus*, D. P. Purpura and M. Yahr, Eds. (Columbia Univ. Press, New York, 1966), p. 47.
18. On the basis of intracellular ionic concentrations in rabbit retina [A. Ames, III, Y. Tsukada, F. Nesbett, *J. Neurochem.* **14**, 145 (1967)] and data on brain amino acids [Y. Tsukada, K. Uemura, S. Hirano, Y. Nagata, in *Comparative Neurochemistry* (Pergamon, Oxford, 1964), p. 178], Ames (personal communication) estimates that there are about 250 meq/liter of cytoplasmic free charges. Comparing the resistivity of rabbit cerebrospinal fluid [G. W. Crile, H. R. Hosmer, A. F. Rowland, *Amer. J. Physiol.* **60**, 59 (1922)] and Tyrode's solution [W. H. Freygang and W. M. Landau, *J. Cell. Comp. Physiol.* **45**, 377 (1955)] with their ionic composition, we estimate (assuming that the chemical estimates pertain about equally to neural and neuroglial cytoplasm) that the internal resistivity is about 60 ohm cm.
19. S. Jacobson and D. A. Pollen, *Science* **161**, 1351 (1968).

20. D. A. Pollen, in *Basic Mechanisms of the Epilepsies*, H. H. Jasper, A. A. Ward, Jr., A. Pope, Eds. (Little, Brown, Boston, 1969), p. 411.
 21. R. Granit, D. Kernell, G. K. Shortess, *J. Physiol. (London)* **168**, 911 (1963); O. D. Creutzfeldt, H. D. Lux, A. C. Nacimiento, *Pfluegers Arch. Gesamte Physiol. Menschen Tiere* **281**, 129 (1964).
 22. A. W. Liley, *J. Physiol. (London)* **134**, 427 (1956); A. Takeuchi and N. Takeuchi, *ibid.* **155**, 46 (1961).
 23. R. S. Bourke, *Exp. Brain Res.* **8**, 232 (1969).
 24. J. Szentagothai, in *Information Processing in the Nervous System*, R. W. Gerard, Ed. (Excerpta Medica, Amsterdam, 1962), p. 119.
 25. D. A. Baylor and J. G. Nicholls, *J. Physiol. (London)* **203**, 555 (1969); *ibid.*, p. 571.
 26. We thank Dr. Charles Feldman for his mathematical suggestions. Supported by PHS grants NB-14353-03 and NB-08632-01 to D.A.P. and NINDB postdoctoral fellowship NB-32383-02 to M.C.T.
- * Present address: Department of Neurology, Boston Veterans Administration Hospital and Boston University School of Medicine, Boston, Mass.

15 September 1969

Neuroglia: Gliosis and Focal Epilepsy

Abstract. *Normal neuroglial cells buffer the extracellular space around neurons and presynaptic terminals against increases in potassium ions. Epileptic foci resulting from brain injury are characterized by areas of intense fibrillary gliosis bordering neuronal tissue. The known pathological changes that occur in gliosis may impair glial control of extracellular potassium ions and lead to excessively excitable neuronal border regions.*

Penfield and co-workers (1) established that the glial scar (alone or as part of a meningocerebral cicatrix) is the irritative source for the focal seizures that develop after anoxic or traumatic brain damage. On the basis of our physiologic findings (2) and on known pathological observations (1), we now propose a pathophysiologic explanation of posttraumatic focal epilepsy.

During neuronal activity K^+ is released into the extracellular space. Increases in extracellular K^+ concentration lead to neuronal depolarization and to an increase in excitability of presynaptic terminals (3). In the normal brain the neuroglial K^+ spatial buffering system (4) transports enough K^+ away from sites of K^+ release to prevent marked (and undesirable) increases in neuronal excitability (2).

Intracerebral and intraventricular injections of potassium salts have long been known to induce seizures (5). Zuckermann and Glaser (6), who em-

ployed chronic intraventricular injection cannulas to enforce local K^+ accumulations to the normal feline dorsal hippocampus, produced seizures with K^+ concentrations as low as 8.1 meq/liter. Short trains of single shocks to the dorsal hippocampus reduced the K^+ concentration necessary for seizure induction to 5.4 meq/liter, and Zuckermann and Glaser noted that increased extracellular K^+ might similarly be a factor in precipitating human seizures.

In gliotic scar formation, protoplasmic astrocytes reorient, proliferate, fill with glial filaments, and become fibrous astrocytes (1). In "epileptogenic scars," fibrous glial cells, in various stages of proliferation and degeneration, border thinned-out gray matter or islands of relatively normal neurons (1). Neuroglial attachments to blood vessels, which are probably required to move K^+ into capillaries, disappear (1). The marked capillary decrease in the border zone (1) suggests a lowered glial metabolic activity. Intermittent ischemia in the glial border zone leads to patches of acute neuroglial degeneration (1). Brain slices of scar tissue from epileptic patients, unlike slices of normal brain, fail to extrude Na^+ and take up K^+ (7).

Structural, vascular, and metabolic defects likely to impair the "passive" K^+ spatial buffering system and the "active" K^+ uptake have thus been demonstrated or are strongly suggested for epileptogenic glial scars. Moreover, human fetal astrocytes raised under relatively anoxic conditions can proliferate but cannot maintain the high internal K^+ concentration needed to establish a high, resting membrane potential, and these cells move relatively little K^+ across their membrane in response to increases in extracellular K^+ (8). An abnormal handling of K^+ in severe gliosis may bear directly on neuronal hyperexcitability in focal epilepsy.

We therefore propose as a hypothesis that a decisive, but by no means the only, factor in the development of posttraumatic focal epilepsy is a degradation of neuroglial function, especially with respect to the spatial buffering of K^+ and active K^+ uptake. As the safety factor with respect to extracellular K^+ control decreases, ordinarily less critical factors (such as hyperthermia, alkalosis, and brain edema) can more easily initiate a given seizure. [If glial cells metabolize neurotrans-

mitters (9), loss of such a function could be an additional factor altering neuronal excitability.] The known effects of anticonvulsants on Na^+ and K^+ balance (10) are consistent with our hypothesis. If deafferentation hypersensitivity is a factor in the development of focal epilepsy, as seems likely (11), it would appear to be a contributory rather than a sufficient factor because, although it would be expected to occur as frequently after clean surgical excision of brain tissue as after brain damage, the surgical procedure is rarely followed by the development of a seizure focus (1). The initiation of focal seizures that may follow surgical traction on a scar might result from interference with neuroglial metabolism secondary to vasospasm (1) and mechanically induced dendritic depolarization, or both, as suggested by Ward (12). Contraction of glial filaments might similarly produce scar traction.

Our hypothesis may offer new approaches to both treatment and prophylaxis of posttraumatic epilepsy. At present, therapy is generally directed against the convulsive activity associated with the scar rather than against the scarring process. Glial scarring is not a static process but may proceed relentlessly over decades (1). Adjacent neurons are victims of a chronic inflammatory process involving vascular elements and reactive gliosis. For this reason, the relevance of developing and testing anti-inflammatory agents for selective effects against gliosis is apparent [see also (13)]. If the fibroblastic invasion and collagen deposition, which occur when the meninges are concomitantly injured, impair K^+ accessibility to glia, then efforts might also be directed against this mesenchymal aspect of scar formation.

Lastly, if development of posttraumatic focal epilepsy is dependent on genetic predisposition (14), we wonder whether the presence or absence of epileptogenicity in association with human glial scars follows genetically determined variations in the extent of scar formation. In any case, a biochemical understanding of the gliotic scar process might allow control of the deleterious extremes of scar formation that lead to focal epileptic discharge.

DANIEL A. POLLEN

MICHAEL C. TRACHTENBERG*

*Neurobiology Laboratory,
Neurosurgical Service, Massachusetts
General Hospital, Boston 02114*